第 43 卷 第 21 期/2023 年 11 月/光学学报 研究论文

光学学报

1064 nm高功率明亮压缩态光场实验制备中的热透镜效应

郭锐[1]，杨文海[2*]，郭咏[1]，姚慧[1]，李丽丽[1]

[1]山西农业大学物理系，山西 太谷 030801；

[2]中国空间技术研究院西安分院，陕西 西安 710000

摘要 本文通过理论和实验分析了1064 nm高功率明亮压缩态光场实验制备过程中，高功率种子光和泵浦光注入光学参量放大器引起的热透镜效应和模式失配。首先根据热透镜理论模型，定量分析了高功率种子光和泵浦光注入光学参量放大器时，周期极化磷酸氧钛钾晶体内部热透镜的等效焦距。然后根据高斯光束与光学谐振腔的模式匹配理论模型，理论分析了高功率种子光和泵浦光与光学参量放大器的模式失配量。最后在高功率明亮压缩态光场正常输出的工作状态下，重新优化种子光和泵浦光与光学参量放大器的模式匹配效率，在种子光功率为500 mW、泵浦光功率为145 mW的条件下，在分析频率3 MHz处，直接测得光功率为200 μW、压缩度为−10.8 dB±0.2 dB的明亮压缩态光场。上述实验结果与有关文献测得的压缩度仅相差0.1 dB，表明在本文实验系统中，高功率种子光和泵浦光引起的热透镜效应对光学参量放大器输出明亮压缩态光场的压缩度基本没有影响。

关键词 量子光学；明亮压缩态；高功率；热透镜效应

中图分类号 O436 **文献标志码** A **DOI**：10.3788/AOS230797

1 引 言

连续变量压缩态光场作为一种重要的量子资源，在量子信息技术领域可用于量子离物传态[1-5]，在量子精密测量领域可用于提升激光干涉仪的探测灵敏度[6-8]。在以上领域的应用中，量子态的保真度和干涉仪的灵敏度均由连续变量压缩态光场的噪声水平直接决定。因此以往的研究重点主要聚焦于提升连续变量压缩态光场的压缩度[9-10]。但是随着研究工作的深入，人们发现连续变量压缩态光场的光功率正成为限制其应用的又一制约因素[11]，所以提升连续变量压缩态光场的光功率显得尤为重要。

根据压缩态光场的平均振幅，压缩态光场可分为压缩真空态光场和明亮压缩态光场。实验制备明亮压缩态光场需要有种子光注入光学参量放大器。高功率明亮压缩态光场与压缩真空态光场最大的区别在于光场振幅不为零，基于这个特性，高功率明亮压缩态光场在量子存储、量子成像和目标探测过程中可以获得更高的保真度、分辨率和灵敏度。从1986年吴令安等[9, 12-15]首次通过参量下转换技术制备得到连续变量压缩态光场起到现在，经过三十多年的发展，连续变量压缩真空态光场的实验制备技术和影响其压缩度提升的物理机制均得到了比较全面的研究。而关于高功率连续变量明亮压缩态光场的研究却较少，尤其最近十几年几乎未见国外报道关于高功率明亮压缩态光场的实验进展，国内只有郑耀辉团队[16-17]于2017年制备得到−12.6 dB的明亮压缩态光场，光场功率约为45 μW。根据相关报道可知，目前限制明亮压缩态光场功率提高的因素主要有三个方面：一是由于光参量放大器(OPA)为欠耦合腔，种子光无法有效耦合注入OPA；二是由于OPA腔内的光学损耗随着种子光功率的增加快速增加；三是高功率种子光注入OPA引起非线性晶体内复杂的热效应和反馈控制环路出现干扰误差信号的噪声。

本文采用半整块驻波腔作为OPA搭建了一套产生高功率明亮压缩态光场的实验系统，在高功率种子光和泵浦光注入OPA的工作条件下，通过热透镜理论模型计算了周期极化磷酸氧钛钾(PPKTP)晶体内热透镜的等效焦距。然后通过定量分析高功率种子光和泵浦光与OPA腔本征模式的模式匹配效率，研究了热透镜效应对OPA输出高功率明亮压缩态光场压缩度的影响。

2 实验系统

如图1所示是产生连续变量高功率明亮压缩态光

收稿日期：2023-04-10；**修回日期**：2023-04-27；**录用日期**：2023-06-26；**网络首发日期**：2023-07-14

基金项目：国家自然科学基金(62001374)

通信作者：*yangwh1@cast504.com

场的实验系统。本实验系统使用山西大学光电研究所研制的高功率1064 nm单频Nd:YVO_4固体激光器，通过外腔倍频过程获得二次谐波作为OPA的泵浦光[18]。实验系统最重要的部分为产生连续变量高功率明亮压缩态光场的OPA，是由非线性晶体PPKTP和凹面腔镜构成的半整块驻波腔。然后是平衡零拍探测装置，可将连续变量高功率明亮压缩态光场和本底光场分为功率相等的两部分，干涉后分别注入平衡零拍探测器。接着通过扫描连续变量高功率明亮压缩态光场和本底光场的相对相位完成压缩态光场某个正交分量噪声功率的测量。此外，为了提升种子光和泵浦光与OPA的模式匹配效率以及连续变量高功率明亮压缩态光场与本底光场的干涉效率，并减少种子光、泵浦光和本底光场携带的相对强度噪声和相位噪声，本文在实验系统种子光路、泵浦光路和本底光路中插入了三镜环形腔模式清洁器。该连续变量高功率明亮压缩态光场实验制备系统中所有光学谐振腔和光场相对相位均采用Pound-Drever-Hall（PDH）技术实现反馈控制。

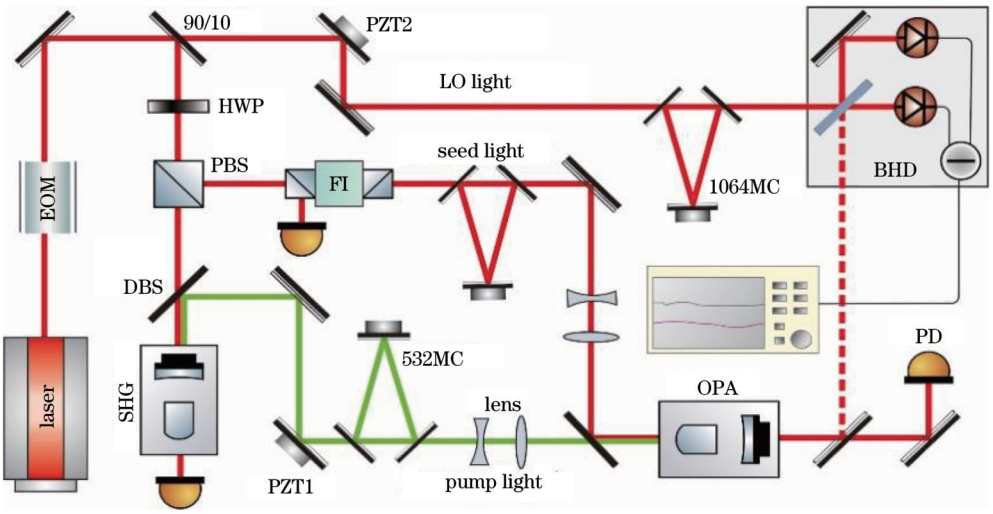

图1　连续变量高功率明亮压缩态光场实验系统

Fig. 1　Experimental system of continuous variable high-power bright squeezed state

3　理论分析与实验过程

非线性晶体的热透镜效应对参量转换过程会产生非常不利的影响[19]，尤其是在本文制备高功率明亮压缩态光场的实验系统中，采用高功率种子光和泵浦光同时注入OPA的方法制备连续变量高功率明亮压缩态光场时[20]。该方法会导致OPA腔内的PPKTP晶体对高功率种子光和泵浦光的非线性吸收增加而出现热沉积，进而在PPKTP晶体内部产生热透镜效应，造成种子光和泵浦光与OPA的模式匹配效率下降。为了提高种子光和泵浦光与OPA的模式匹配效率，提升高功率明亮压缩态光场的压缩度，需要通过理论计算定量分析OPA工作状态下PPKTP晶体的热透镜焦距，然后通过实验重新调整种子光和泵浦光光路中的透镜组，改变种子光和泵浦光的腰斑半径和位置，以实现种子光和泵浦光与PPKTP晶体产生热透镜后的OPA的本征模式重新匹配。

根据文献[21]可知，PPKTP晶体内产生的热透镜可以等效为一般的薄透镜，其焦距可以表示为

$$f_{\mathrm{sum}}=\frac{f_1 f_2}{f_1+f_2}, \tag{1}$$

$$f_1=\frac{\pi K\omega_1^2}{P_{\mathrm{seed}}(\mathrm{d}n/\mathrm{d}T)}\times\frac{1}{1-\mathrm{e}^{-2\alpha_1 l}}, \tag{2}$$

$$f_2=\frac{\pi K\omega_2^2}{P_{\mathrm{pump}}(\mathrm{d}n/\mathrm{d}T)}\times\frac{1}{1-\mathrm{e}^{-2\alpha_2 l}}, \tag{3}$$

式中：$K=13\ \mathrm{W/(m\cdot K)}$是PPKTP晶体的热导率；$\omega_1$和$\omega_2$分别是OPA无热透镜效应时OPA腔内种子光和泵浦光对应本征模式的腰斑半径；P_{seed}和P_{pump}分别是注入OPA的种子光功率和泵浦光功率；$\mathrm{d}n/\mathrm{d}T=1.6\times10^{-5}\ \mathrm{K^{-1}}$是PPKTP晶体的热光系数；$\alpha_1=0.06\ \mathrm{cm^{-1}}$和$\alpha_2=0.048\ \mathrm{cm^{-1}}$分别是PPKTP晶体对种子光和泵浦光的吸收系数[20,22]；l是PPKTP晶体的长度。

本文实验系统OPA采用有利于产生宽频带压缩态光场的双凹型半整块驻波腔[23]，其$ABCD$矩阵可以表示为

$$\begin{pmatrix} A & B \\ C & D \end{pmatrix}=\begin{pmatrix} 1 & L_1/n \\ 0 & 1 \end{pmatrix}\times\begin{pmatrix} 1 & 0 \\ 1/f & 1 \end{pmatrix}\times\begin{pmatrix} 1 & L_2/n \\ 0 & 1 \end{pmatrix}\times\begin{pmatrix} 1 & L_3 \\ 0 & 1 \end{pmatrix}\times\begin{pmatrix} 1 & 0 \\ 2/R_2 & 1 \end{pmatrix}\times\begin{pmatrix} 1 & L_3 \\ 0 & 1 \end{pmatrix}\times\begin{pmatrix} 1 & L_2/n \\ 0 & 1 \end{pmatrix}\times\begin{pmatrix} 1 & 0 \\ 1/f & 1 \end{pmatrix}\times\begin{pmatrix} 1 & L_1/n \\ 0 & 1 \end{pmatrix}\times\begin{pmatrix} 1 & 0 \\ 2/R_1 & 1 \end{pmatrix}, \tag{4}$$

式中：R_1是PPKTP晶体前端凸面的曲率半径；L_1和L_2分别是OPA腔模腰斑到PPKTP晶体前端凸面和后端平面的距离；n是PPKTP晶体对种子光或泵浦光的折射率，分别为$n_1=1.83$，$n_2=1.89$；L_3是PPKTP晶体后端平面与输出腔镜之间的距离；R_2是OPA输出腔镜的曲率半径。

本文实验系统OPA采用的双凹型半整块驻波腔的主要参数如下：PPKTP晶体尺寸为1 mm×2 mm×10 mm；晶体前端加工有凸面，其曲率半径为12 mm，镀532 nm减反膜和1064 nm高反膜；晶体后端为平面，镀532 nm和1064 nm减反膜；晶体后端平面与输出腔镜之间的距离为25 mm，输出腔镜曲率半径为30 mm，镀1064 nm部分反射膜和532 nm高反膜，其中部分反射膜的反射率为88%。根据上述参数和式(4)可以算出，无热透镜效应时OPA腔内种子光和泵浦光对应本征模式的腰斑半径分别为ω_1=31.3 μm和ω_2=19.9 μm，种子光和泵浦光对应腔模腰斑距PPKTP晶体前端凸面的距离分别为L_1=0.75 mm和L_1'=0.47 mm。根据式(1)～(3)，在泵浦功率为145 mW、种子光功率为500 mW时，可以计算出PPKTP晶体内热透镜的等效焦距约为182 mm，代入式(4)可以算出OPA存在热透镜效应时，OPA腔内种子光和泵浦光对应本征模式的腰斑半径分别为ω_1'=30.6 μm和ω_2'=19.4 μm，种子光和泵浦光对应腔模腰斑距PPKTP晶体前端凸面的距离分别为L_1=0.68 mm和L_1'=0.43 mm。由上述计算结果可知，PPKTP晶体内部产生的热透镜效应使OPA腔内种子光和泵浦光对应本征模式的腰斑半径和位置均发生改变。

为了定量分析热透镜引起的OPA腔内种子光和泵浦光对应本征模式的变化量，引入文献[24]中关于高斯光束与光学谐振腔高效模式匹配的理论模型，可以将种子光和泵浦光与OPA腔TEM_{00}本征模式的模式匹配效率表示为

$$\kappa_{00}=\frac{16\prod_{\alpha=x,y}\left[\int_0^L\frac{1}{\omega_\alpha^2(z)+\omega_{\alpha,e}^2(z)}\mathrm{d}z\right]^2}{\prod_\alpha\left[\int_0^L\frac{1}{\omega_\alpha^2(z)}\mathrm{d}z\right]\left[\int_0^L\frac{1}{\omega_{\alpha,e}^2(z)}\mathrm{d}z\right]}, \tag{5}$$

式中：x、y和z分别表示水平方向和竖直方向的坐标轴；L是OPA腔长；$\omega_\alpha(z)$是种子光或泵浦光在OPA腔内任意位置的光斑半径，可以表示为

$$\omega_\alpha^2(z)=\omega_{\alpha0}^2\left[1+\left(\frac{z-z_\alpha}{z_{\alpha0}}\right)\right]^2, \tag{6}$$

$$z_{\alpha0}=\pi\omega_{\alpha0}^2/\lambda, \tag{7}$$

式中：$\omega_{\alpha0}$是种子光或泵浦光在OPA腔内的腰斑半径；λ是种子光或泵浦光的波长。同理，$\omega_{\alpha,e}(z)$是OPA腔本征模式在腔内任意位置的半径，可以表示为

$$\omega_{\alpha,e}^2(z)=\omega_{\alpha,e0}^2\left[1+\left(\frac{z-z_{\alpha,e}}{z_{\alpha,e0}}\right)\right]^2, \tag{8}$$

$$z_{\alpha,e0}=\pi\omega_{\alpha,e0}^2/\lambda, \tag{9}$$

式中，$\omega_{\alpha,e0}$是OPA腔本征模式的腰斑半径。将上述计算结果代入式(5)～(9)可以算出，在泵浦功率为145 mW、种子光功率为500 mW时，高功率种子光和泵浦光与OPA腔的模式匹配效率分别下降到99.8%和99.9%。根据上述理论分析与计算结果可知，在上述工作条件下，OPA输出高功率明亮压缩态光场时，PPKTP晶体的热透镜效应不会导致高功率种子光和泵浦光与OPA腔的模式匹配效率显著下降。当进一步增加种子光和泵浦光的功率时，注入OPA腔内的高功率种子光和泵浦光会在PPKTP晶体中引起更加剧烈且复杂的热沉积过程(如绿光诱导红外吸收效应)，由于热透镜效应加剧的趋势不是线性的，而可能是近似指数的增加趋势，因此热透镜效应将会导致泵浦光和OPA腔的模式匹配效率急剧下降，在模式匹配效率明显降低的工作状态下，热透镜效应就会显著影响OPA输出明亮压缩态光场的压缩度。

压缩态光场的压缩度可以表示为

$$S=10\lg V_\mathrm{s}, \tag{10}$$

式中，V_s是压缩态光场正交压缩分量的归一化噪声方差，由下式给出：

$$V_\mathrm{s}=1\pm\frac{4(1-l_\mathrm{tot})\sqrt{P_\mathrm{sh}/P_\mathrm{th}}}{\left(1\mp\sqrt{P_\mathrm{sh}/P_\mathrm{th}}\right)^2+4\left(f/\kappa\right)^2}, \tag{11}$$

式中：P_sh为泵浦功率；P_th为OPA阈值；f为分析频率；κ为OPA线宽；l_tot为压缩态光场的总光学损耗。热透镜效应导致高功率种子光和泵浦光与OPA腔的模式匹配效率降低，主要影响注入到OPA腔内的种子光功率和泵浦光功率。理论上注入OPA腔内的种子光功率变化对明亮压缩态光场的压缩度不会产生影响，所以只需考虑注入OPA腔内的泵浦光功率变化对明亮压缩态光场压缩度的影响。考虑到模式匹配效率对注入OPA腔内泵浦光功率的影响，可以将OPA腔内泵浦光功率表示为

$$P_{in}=\kappa_{00}P_{sh}。\tag{12}$$

根据式(4)～(10)可以推导出OPA腔内热透镜焦距与泵浦光和OPA腔模式匹配效率之间的定量关系，将式(12)代入式(11)可得出泵浦光和OPA腔模式匹配效率与明亮压缩态光场压缩度之间的定量关系，进而可以推导得到OPA腔内热透镜焦距与明亮压缩态光场压缩度之间的定量关系。

微调种子光和泵浦光光路中焦距为25 mm的凸透镜和焦距为−50 mm的凹透镜的位置，使高功率种子光和泵浦光与OPA腔的模式匹配效率达到最高，然后采用罗德斯瓦茨公司的Signal & Spectrum Analyzer·2 Hz to 13 GHz频谱仪对OPA输出高功率明亮压缩态光场的压缩度进行测量，最终在分析频率3 MHz处，直接测得光功率为200 μW、压缩度为−10.8 dB±0.2 dB的高功率明亮压缩态光场，其噪声功率谱如图2所示，与文献[20]报道的高功率明亮压缩态光场的指标基本相等。

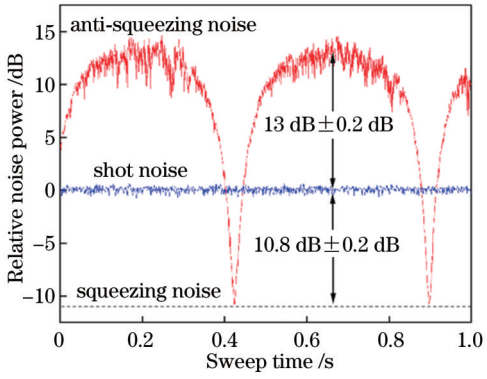

图2　高功率明亮压缩态光场的噪声功率谱[分析频率3 MHz处分辨率带宽(RBW)为300 kHz，视频带宽(VBW)为200 Hz]

Fig. 2　Noise power spectrum of high-power bright squeezed state at analysis frequency of 3 MHz, with resolution bandwidth (RBW) of 300 kHz and video bandwidth (VBW) of 200 Hz

根据文献[20]所述实验系统的工作条件可知，在OPA腔内存在热透镜，且在未优化高功率种子光和泵浦光与OPA腔的模式匹配的条件下，测得−10.7 dB±0.2 dB的高功率明亮压缩态光场。通过与本文测得的高功率明亮压缩态光场的压缩度对比，可以推断出，在PPKTP晶体内部存在热透镜效应时，高功率种子光和泵浦光与OPA腔的模式匹配效率未出现明显下降，所以热透镜效应对高功率明亮压缩态光场的压缩度影响较小，即本文实验系统在该工作条件下，OPA腔内PPKTP晶体的热透镜效应对高功率明亮压缩态光场的压缩度基本没有影响。

此外，本文还对比分析了实验制备压缩真空态光场过程中光参量振荡器(OPO)腔内热透镜效应与实验制备高功率明亮压缩态光场过程中OPA腔内热透镜效应对压缩态光场压缩度的影响。根据上述分析结果可知，影响高功率明亮压缩态光场压缩度的主要因素是：热透镜效应导致的泵浦光与OPA腔的模式匹配效率降低，使得注入OPA腔的泵浦光功率下降。众所周知，实验制备明亮压缩态光场与压缩真空态光场均需高功率泵浦光注入OPA腔和OPO腔，最大的区别在于是否有种子光注入OPA腔和OPO腔。有种子光注入OPA腔时，OPA输出的是明亮压缩态光场；没有种子光注入OPO腔时，OPO输出的是压缩真空态光场。由此可知，热透镜效应影响压缩真空态光场压缩度的主要因素仍然是：热透镜效应导致泵浦光与OPA腔的模式匹配效率降低，使得注入OPA腔的泵浦光功率下降。唯一的区别在于，实验制备压缩真空态光场时，OPO腔内PPKTP晶体中没有叠加种子光产生的热透镜效应，所以OPO腔内的热透镜效应会比制备高功率明亮压缩态光场的OPA腔内的热透镜效应要弱一些，从而导致泵浦光与OPO腔的模式匹配效率降低的幅度会更小一些。综上所述，可得出以下结论：同等实验条件下，在不考虑PPKTP晶体中高功率种子光和泵浦光之间产生的其他效应(如绿光诱导红外吸收效应)，仅考虑热透镜效应的情况下，理论上OPO产生的压缩真空态光场的压缩度会比OPA产生的高功率明亮压缩态光场的压缩度更高一些。

4　结　　论

本文通过实验和理论研究了连续变量高功率明亮压缩态光场实验系统中，高功率种子光和泵浦光在PPKTP晶体内部产生的热透镜效应。通过热透镜理论模型和模式匹配理论模型，定量分析了PPKTP晶体内部热透镜的等效焦距以及种子光和泵浦光与OPA的模式失配量。首先通过理论分析和计算得知，PPKTP晶体内热透镜的等效焦距约为182 mm，实验系统在该工作状态下，由于PPKTP晶体内部产生了热透镜效应，高功率种子光和泵浦光与OPA腔的模式匹配效率分别下降到99.8%和99.9%；然后通过重新优化高功率种子光和泵浦光与OPA腔的模式匹配，最后在种子光功率为500 mW、泵浦光功率为145 mW的条件下，在分析频率3 MHz处，获得光功率为200 μW、压缩度为−10.8 dB±0.2 dB的高功率明亮压缩态光场。以上研究结果表明，在本文制备高功率明亮压缩态光场的工作条件下，高功率种子光和泵浦光注入OPA引起PPKTP晶体内部产生的热透镜效应不足以导致高功率种子光和泵浦光与OPA腔的模式匹配效率显著下降，所以基本不会影响OPA输出明亮压缩态光场的压缩度。

参　考　文　献

[1] Furusawa A, Sorensen J L, Braunstein S L, et al. Unconditional quantum teleportation[J]. Science, 1998, 282

(5389): 706-709.

[2] 王少锋, 项晓, 董瑞芳, 等. 量子光频梳产生实验研究[J]. 光学学报, 2018, 38(10): 1027003.
Wang S F, Xiang X, Dong R F, et al. Research on experimental generation of quantum optical frequency comb[J]. Acta Optica Sinica, 2018, 38(10): 1027003.

[3] Wu Y M, Wang Q W, Tian L, et al. Multi-channel multiplexing quantum teleportation based on the entangled sideband modes[J]. Photonics Research, 2022, 10(8): 1909-1914.

[4] Shi S P, Tian L, Wang Y J, et al. Demonstration of channel multiplexing quantum communication exploiting entangled sideband modes[J]. Physical Review Letters, 2020, 125(7): 070502.

[5] Braunstein S L, van Loock P. Quantum information with continuous variables[J]. Reviews of Modern Physics, 2005, 77(2): 513-577.

[6] 刘翊钊, 左小杰, 闫智辉, 等. 基于光学参量放大器的量子干涉仪的分析[J]. 光学学报, 2022, 42(3): 0327013.
Liu Y Z, Zuo X J, Yan Z H, et al. Analysis of quantum interferometer based on optical parametric amplifier[J]. Acta Optica Sinica, 2022, 42(3): 0327013.

[7] Tse M, Yu H C, Kijbunchoo N, et al. Quantum-enhanced advanced LIGO detectors in the era of gravitational-wave astronomy[J]. Physical Review Letters, 2019, 123(23): 231107.

[8] Grote H, Danzmann K, Dooley K L, et al. First long-term application of squeezed states of light in a gravitational-wave observatory[J]. Physical Review Letters, 2013, 110(18): 181101.

[9] Sun X C, Wang Y J, Tian L, et al. Detection of 13.8 dB squeezed vacuum states by optimizing the interference efficiency and gain of balanced homodyne detection[J]. Chinese Optics Letters, 2019, 17(7): 072701.

[10] Vahlbruch H, Mehmet M, Danzmann K, et al. Detection of 15 dB squeezed states of light and their application for the absolute calibration of photoelectric quantum efficiency[J]. Physical Review Letters, 2016, 117(11): 110801.

[11] Li B B, Hoff U B, Madsen L S, et al. Quantum enhanced optomechanical magnetometry[J]. Optica, 2018, 5(7): 850-856.

[12] Wu L A, Kimble H J, Hall J L, et al. Generation of squeezed states by parametric down conversion[J]. Physical Review Letters, 1986, 57(20): 2520-2523.

[13] McKenzie K, Mikhailov E E, Goda K, et al. Quantum noise locking[J]. Journal of Optics B: Quantum and Semiclassical Optics, 2005, 7(10): S421-S428.

[14] Vahlbruch H, Chelkowski S, Hage B, et al. Coherent control of vacuum squeezing in the gravitational-wave detection band[J]. Physical Review Letters, 2006, 97: 011101.

[15] Shi S P, Wang Y J, Yang W H, et al. Detection and perfect fitting of 13.2 dB squeezed vacuum states by considering green-light-induced infrared absorption[J]. Optics Letters, 2018, 43(21): 5411-5414.

[16] 秦忠忠, 王美红, 马荣, 等. 压缩态光场及其应用研究进展[J]. 激光与光电子学进展, 2022, 59(11): 1100001.
Qin Z Z, Wang M H, Ma R, et al. Progress of the squeezed states of light and their application[J]. Laser & Optoelectronics Progress, 2022, 59(11): 1100001.

[17] Yang W H, Shi S P, Wang Y J, et al. Detection of stably bright squeezed light with the quantum noise reduction of 12.6 dB by mutually compensating the phase fluctuations[J]. Optics Letters, 2017, 42(21): 4553-4556.

[18] 田宇航, 王俊萍, 杨文海, 等. 集成量子压缩光源中 MgO: $LiNbO_3$ 晶体倍频系统研究[J]. 中国激光, 2020, 47(11): 1108001.
Tian Y H, Wang J P, Yang W H, et al. Frequency doubling system for integrated quantum squeezed light source based on MgO: $LiNbO_3$ crystal[J]. Chinese Journal of Lasers, 2020, 47(11): 1108001.

[19] 王海龙, 杨慧琦, 苏静, 等. 基于单共振光学参量振荡器实现近红外到中红外激光输出的实验研究[J]. 中国激光, 2022, 49(18): 1801005.
Wang H L, Yang H Q, Su J, et al. Experimental study on near-infrared to mid-infrared laser output based on single resonant optical parametric oscillator[J]. Chinese Journal of Lasers, 2022, 49(18): 1801005.

[20] 郭锐, 杨文海, 郭咏, 等. 1064 nm高功率明亮压缩态光场制备实验中绿光诱导红外吸收效应[J]. 光学学报, 2023, 43(10): 1027001.
Guo R, Yang W H, Guo Y, et al. Green light-induced infrared absorption effect in preparation experiment of high-power bright squeezed state light field of 1064 nm[J]. Acta Optica Sinica, 2023, 43(10): 1027001.

[21] Innocenzi M E, Yura H T, Fincher C L, et al. Thermal modeling of continuous-wave end-pumped solid-state lasers[J]. Applied Physics Letters, 1990, 56(19): 1831-1833.

[22] 张晓莉, 王庆伟, 姚文秀, 等. 热透镜效应对半整块腔型中二次谐波过程的影响[J]. 物理学报, 2022, 71(18): 184203.
Zhang X L, Wang Q W, Yao W X, et al. Influence of thermal lens effect on second harmonic process in semi-monolithic cavity [J]. Acta Physica Sinica, 2022, 71(18): 184203.

[23] 王俊萍, 张文慧, 李瑞鑫, 等. 宽频带压缩态光场光学参量腔的设计[J]. 物理学报, 2020, 69(23): 234204.
Wang J P, Zhang W H, Li R X, et al. Design of optical parametric cavity for broadband squeezed light field[J]. Acta Physica Sinica, 2020, 69(23): 234204.

[24] Uehara N, Gustafson E K, Fejer M M, et al. Modeling of efficient mode-matching and thermal-lensing effect on a laser-beam coupling into a mode-cleaner cavity[J]. Proceedings of SPIE, 1997, 2989: 57-68.

Thermal Lens Effect in Experimental Preparation of 1064 nm High-Power Bright Squeezed State

Guo Rui[1], Yang Wenhai[2*], Guo Yong[1], Yao Hui[1], Li Lili[1]

[1]*Department of Physics, Shanxi Agricultural University, Taigu* 030801, *Shanxi, China*;

[2]*China Academy of Space Technology (Xi´an), Xi´an* 710000, *Shaanxi, China*

Abstract

Objective As an important quantum resource, the squeezed state can not only be employed for quantum teleportation in quantum information technology but also can be adopted to improve the detection sensitivity of laser interferometer in quantum precision measurement. In the above applications, the quantum state fidelity and interferometer sensitivity are directly determined by the noise level of the squeezed state. Therefore, previous research focuses on improving the squeezing degree of squeezed state. However, with the deepening research, the optical power of the squeezed state is another factor limiting its application, and thus it is important to improve the optical power of the squeezed state.

Methods The experimental preparation system is built as shown in Fig. 1. The most important part of the experimental system is the optical parametric amplifier (OPA), which generates the high-power bright squeezed state. The OPA is a semi-monolithic standing cavity composed of periodically poled $KTiOPO_4$ (PPKTP) crystal and concave cavity mirror. Then the balanced homodyne detection device can divide the high-power bright squeezed state and the local oscillator into two parts with equal power, and inject the balanced homodyne detector respectively after interference. The squeezing degree is measured by scanning the relative phase of the high-power bright squeezed state and the local oscillator.

The thermal lens effect of PPKTP crystal exerts a very adverse effect on the parametric conversion. The method of simultaneously injecting high-power seed light and pump light into OPA is adopted especially in the experimental system of preparing high-power bright squeezed state. This method will increase the nonlinear absorption of high-power seed light and pump light, resulting in thermal deposition and then a thermal lens effect in the PPKTP crystal. Finally, the mode matching efficiency of the seed light and pump light with OPA is decreased. To improve the mode matching efficiency of seed light and pump light with OPA and enhance the squeezing degree, we should quantitatively analyze the thermal lens focal length of PPKTP crystal under OPA working state and then adjust the lens group in the optical path of seed light and pump light to realize the rematch of seed light and pump light with the intrinsic mode of OPA with thermal lens effect.

Results and Discussions According to the experimental parameters and theoretical calculation, under the OPA without thermal lens effect, the waist radii corresponding to the seed light and pump light in the OPA cavity are ω_1=31.3 μm and ω_2=19.9 μm respectively. The distance between the waist and the front convex surface of PPKTP crystal is L_1=0.75 mm and L_1'=0.47 mm respectively. When the pump light power is 145 mW and the seed light power is 500 mW, the equivalent focal length of the thermal lens in the PPKTP crystal can be calculated to be about 182 mm. Under the OPA with thermal lens effect, the waist radii corresponding to seed light and pump light in OPA are ω_1'=30.6 μm and ω_2'=19.4 μm respectively. The distance between the waist and the front convex surface of PPKTP crystal corresponding to seed light and pump light is L_1=0.68 mm and L_1'=0.43 mm respectively. The above calculation results show that the thermal lens changes the intrinsic mode waist of OPA. The theoretical calculation results confirm that the mode matching efficiency of seed light and pump light with OPA decreases to 99.8% and 99.9% respectively, while the OPA produces bright squeezed light with high power.

When the powers of seed light and pump light are further increased, the high-power seed light and pump light will cause more intense and complex thermal deposition in the PPKTP crystal (such as the green light-induced infrared absorption effect). This is because the intensification trend of the thermal lens effect is not linear, but may be an approximate exponential increase. Therefore, the thermal lens effect will cause sharply decreased mode matching efficiency between the seed light (the pump light) and the OPA. Thus, the thermal lens effect will significantly affect the squeezing degree. The mode matching efficiency of seed light and pump light with OPA is reduced by the thermal lens effect, which mainly affects the power of seed light and pump light injected into OPA. Theoretically, the change of seed light power has no effect on the squeezing degree. Therefore, it is only necessary to consider the influence of pump light power in OPA on the squeezing degree of the bright squeezed state. Finally, according to Eqs. (4)-(12), the quantitative relationship between the focal length of the thermal lens and the squeezing degree can be derived.

According to the working conditions of the experimental system in Ref. [20], there is a thermal lens in the OPA, and the high-power bright squeezed state of −10.7 dB±0.2 dB is measured without optimizing the mode matching of seed

light and pump light with the OPA. The squeezing degree comparison reveals that with the thermal lens effect, the mode matching efficiency reduction of seed light and pump light with the OPA has little effect on the squeezing degree. This means the thermal lens effect in OPA has little effect on the squeezing degree of the high-power bright squeezed state. Additionally, the different effects of thermal lens effect on the squeezing degree of high-power bright squeezed state and squeezed vacuum state are compared and analyzed. Meanwhile, the following conclusions are drawn. In the same experimental conditions, the squeezing degree of the squeezed vacuum state generated by optical parametric oscillator (OPO) will be higher than that of the high-power bright squeezed state generated by OPA if other effects between the high-power seed light and pump light in PPKTP crystal are not considered, with the thermal lens effect only considered.

Conclusions In the high-power bright squeezed state experiment system, the thermal lens effect of high-power seed light and pump light in PPKTP crystal is studied experimentally and theoretically. The equivalent focal length of the thermal lens and the mode mismatch between seed light and OPA, and between pump light and OPA are quantitatively analyzed by the theoretical model of thermal lens and mode matching. The equivalent focal length of the thermal lens in the PPKTP crystal can be calculated as 182 mm by theoretical analysis and calculation. In the working condition of the experimental system, due to the thermal lens generated in the PPKTP crystal, the mode matching efficiency of the high-power seed light and pump light with the OPA decreases to 99.8% and 99.9% respectively. Then the mode matching of high-power seed light and pump light with the OPA cavity is re-optimized. Finally, under the seed light power of 500 mW and pump light power of 145 mW, a bright squeezed state with power of 200 μW and squeezing degree of −10.8 dB±0.2 dB is obtained at the analysis frequency of 3 MHz. The results show that during the preparation of a high-power bright squeezed state, the squeezing degree of the high-power bright squeezed state is basically unaffected, since the thermal lens effect in PPKTP crystal caused by the high-power seed light and pump light does not significantly reduce the mode matching efficiency of the high-power seed light and pump light with OPA.

Key words quantum optics; bright squeezed state; high power; thermal lens effect